Slow dynamics and glass transition in simulated free-standing polymer films: a possible relation between global and local glass transition temperatures

2007 J. Phys.: Condens. Matter 19 205119

(http://iopscience.iop.org/0953-8984/19/20/205119)

IOP PUBLISHING JOURNAL OF PHYSICS: CONDENSED MATTER

J. Phys.: Condens. Matter **19** (2007) 205119 (11pp) doi:10.1088/0953-8984/19/20/205119

Slow dynamics and glass transition in simulated free-standing polymer films: a possible relation between global and local glass transition temperatures

S Peter[1], H Meyer[1], J Baschnagel[1] and R Seemann[2]

[1] Institut Charles Sadron, 6 rue Boussingault, 67083 Strasbourg Cedex, France
[2] Max Planck Institute for Dynamics and Self-Organization, D-37018 Göttingen, Germany

E-mail: peter@ics.u-strasbg.fr and baschnag@ics.u-strasbg.fr

Received 17 October 2006, in final form 3 January 2007
Published 25 April 2007
Online at stacks.iop.org/JPhysCM/19/205119

Abstract

We employ molecular dynamics simulations to explore the influence that the surface of a free-standing polymer film exerts on its structural relaxation when the film is cooled toward the glass transition. Our simulations are concerned with the features of a coarse-grained bead-spring model in a temperature regime above the critical temperature T_c of mode-coupling theory. We find that the film dynamics is spatially heterogeneous. Monomers at the free surface relax much faster than they would in the bulk at the same temperature T. The fast relaxation of the surface layer continuously turns into bulk-like relaxation with increasing distance y from the surface. This crossover remains smooth for all T, but its range grows on cooling. We show that it is possible to associate a gradient in critical temperatures $T_c(y)$ with the gradient in the relaxation dynamics. This finding is in qualitative agreement with experimental results on supported polystyrene (PS) films (Ellison and Torkelson 2003 *Nat. Mater.* **2** 695). Furthermore we show that the y dependence of $T_c(y)$ can be expressed in terms of the depression of $T_c(h)$—the global T_c for a film of thickness h—if we assume that $T_c(h)$ is the arithmetic mean of $T_c(y)$ and parameterize the depression of $T_c(h)$ by $T_c(h) = T_c/(1 + h_0/h)$, a formula suggested by Herminghaus *et al* (2001 *Eur. Phys. J.* E **5** 531) for the reduction of the glass transition temperature in supported PS films. We demonstrate the validity of this formula by comparing our simulation results to results from other simulations and experiments.

1. Introduction

Experiments [1–11], computer simulations [12–21] and theoretical approaches [22–27] have recently been used to explore the phenomenology and underlying mechanism of the glass transition in spatial confinement. Typically, these studies report deviations from bulk behaviour

if a glass former is confined to nanoscopic dimensions. The origin of these deviations is, however, not fully understood. Proposed explanations involve confinement and/or interfacial effects (see [28–31] for reviews). If the glass transition in the bulk was connected to the growth of a correlation length ξ_g, this growth should be truncated by the spatial confinement, entailing a depression of the glass transition temperature T_g [32]. On the other hand, the confinement also creates environments for nearby particles which differ from those of the bulk. Such interfacial effects may have different contributions resulting, for example, from specific particle–substrate interactions, confinement-induced changes of the liquid structure and polymer chain conformations, or density variations. As ξ_g does not become much larger than the molecular diameter on cooling—ξ_g attains a few nanometres at T_g [32]—it is difficult to clearly disentangle confinement and interfacial effects [30]. In many cases, interfacial effects appear to be dominant.

Computer simulations of model systems provide an example of the importance of interfacial effects. The simulations demonstrate that deviations from bulk behaviour may originate from the particle–substrate interaction. For instance, strong particle–substrate interactions—due to preferential attraction or strong caging of the liquid in cavities of the substrate—can temporarily trap particles close to the confining walls and lead to an overall slower dynamics than in the bulk [16, 17, 19, 20]. On the other hand, for free-standing films, i.e. for systems with two liquid–vacuum interfaces, faster than bulk dynamics and, along with that, a depression of T_g is found [12, 16, 21, 33]. Furthermore, the simulations suggest that the dynamics of the confined liquid is very heterogeneous at low temperature T. Near the interface relaxation times may differ by orders of magnitude from those of the bulk. This fast or slow relaxation—depending on the boundary condition—continuously turns into bulk-like relaxation with increasing distance from the interface. For all T this crossover remains continuous, but its range grows on cooling so that the wall-induced perturbations may propagate across the entire liquid at low T or for strong confinement (see [31] for a review).

In this paper we provide further evidence for this scenario by molecular dynamics simulations of free-standing polymer films. In agreement with recent experiments on supported polystyrene films [9] we find that the free surface gives rise to a local glass transition temperature which decreases with decreasing distance to the surface. We show that this distance dependence can be understood from the average behaviour of the film, that is, from the depression of T_g with decreasing film thickness, which is well described by a parametrization suggested by Herminghaus and co-workers [4].

The remainder of this paper is organized as follows. Section 2 describes the model used to simulate free-standing polymer films. Section 3 discusses the simulation results and section 4 presents our conclusions.

2. Model

A polymer melt is a dense disordered system consisting of chain molecules. We model the polymer chains by a bead-spring model [34] in which each chain has N monomers (monodisperse melt). The monomers interact by two types of potential, depending on whether they are bonded nearest neighbours along the chain backbone or not bonded to each other. Nonbonded interactions are represented by a Lennard-Jones (LJ) potential that is truncated at the cut-off radius $r_c = 2.3\sigma$ ($\simeq 2r_{min}$, r_{min} being the minimum of the LJ potential) and shifted to 0,

$$U_{LJ}(r) = 4\epsilon\left[\left(\frac{\sigma}{r}\right)^{12} - \left(\frac{\sigma}{r}\right)^{6}\right] - \text{constant}, \qquad r \leqslant r_c. \tag{1}$$

$U_{\mathrm{LJ}}(r)$ is not considered between nearest neighbours along the chain. These monomers are connected to each other by a harmonic potential with equilibrium distance $r_0 = 0.967\sigma$ and spring constant $k = 1111\epsilon/\sigma^2$,

$$U_{\mathrm{bond}}(r) = \frac{k}{2}(r - r_0)^2. \tag{2}$$

In the following we will use LJ units—that is, $\epsilon = 1$, $\sigma = 1$ and mass $m = 1$. Then, temperature T is measured in units of ϵ/k_{B} (Boltzmann constant $k_{\mathrm{B}} = 1$), and time t in units of $(m\sigma^2/\epsilon)^{1/2}$.

The value of k in equation (2) is large enough to prevent chains from crossing each other in the course of the simulation. This allows for the formation of entanglements. The entanglement length N_{e} of our model is $N_{\mathrm{e}} \approx 32$ [35, 36]. In the following, we re-analyse the results for nonentangled melts ($N = 10$) from [33] and also discuss new data for weakly entangled chains ($N = 64$).

These results were obtained from molecular dynamics (MD) simulations of free-standing polymer films under isothermal (DPD thermostat) and isobaric (Andersen barostat) conditions [37]. In our model, the films have two polymer–vacuum interfaces. As no external forces act on the monomers at these interfaces, the pressure p vanishes. Thus, we performed MD simulations in thermal equilibrium at $p = 0$ for various T above the critical temperature T_{c} of mode-coupling theory for the polymer films (see below). More details about the simulation technique, the method used to prepare the films and the equilibration of the systems may be found in [33].

3. Results

In this section we explore the structural relaxation of free-standing polymer films on cooling toward T_{c}. The simulation offers two ways of performing this study: either by a layer-wise resolution of the dynamics or by determining averages over the film. We will present examples for both approaches and begin our discussion with the latter.

3.1. Dynamic properties averaged over the film

Among the convenient quantities for characterizing the dynamics are mean square displacements (MSDs)—for example, the MSD of the middle monomer of a chain,

$$g_1(t) = \left\langle \left[\vec{r}^{\,\parallel}_{N/2}(t) - \vec{r}^{\,\parallel}_{N/2}(0)\right]^2 \right\rangle. \tag{3}$$

Here $\vec{r}^{\,\parallel}_{N/2}(t)$ denotes the position, parallel to the wall, of the middle monomer at time t. We only consider displacements within the plane of the film because motion in a parallel direction is not bound by the finite film thickness. This allows for a comparison of the long time dynamics with the corresponding bulk system.

Figure 1 depicts $g_1(t)$ at $T = 0.44$ for two free-standing films and for the bulk. The dynamics of the bulk and films are qualitatively similar. We can identify the following regimes with increasing t. At short times the motion is ballistic ($g_1(t) \sim t^2$). For longer times the MSD increases more weakly, particularly in the bulk where a plateau-like regime emerges. This regime corresponds to displacements of the order of 10% of the monomer diameter. Monomers are thus temporarily trapped in the 'cage' formed by their neighbours. Both in the bulk and the films this caging becomes more pronounced on cooling, thus shifting the onset of large monomer displacements and the attendant full structural relaxation of the system to increasingly longer times [31, 33]. When the monomers escape from their cage the motion does

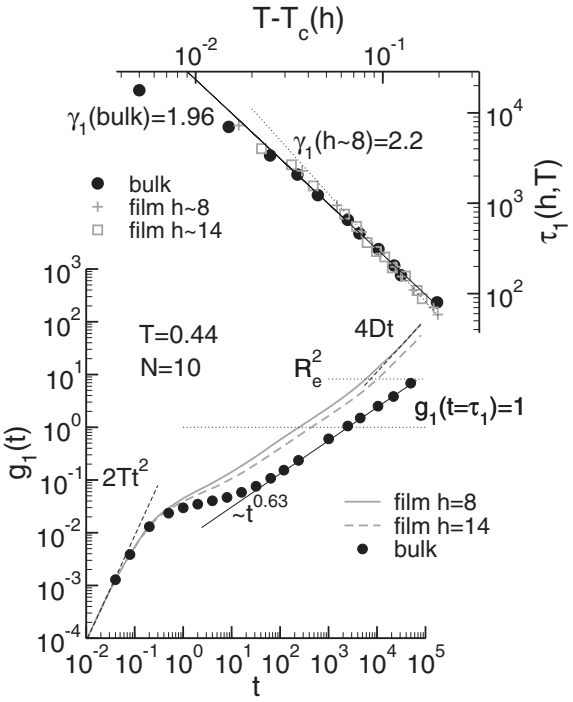

Figure 1. $g_1(t)$ (equation (3)) and $\tau_1(h, T)$ (equation (4)) for $N = 10$. Left ordinate: log–log plot of $g_1(t)$ versus t at $T = 0.44$ for the bulk and two free-standing films of thicknesses $h = 8$ and 14. In the films, the MSDs are measured in a direction parallel to the wall and the bulk data are multiplied by 2/3 to account for the difference in the number of directions compared to the films. The dotted horizontal lines show the definition of the relaxation time τ_1 (equation (4)) and the bulk end-to-end distance within the plane ${R_e}^2 \simeq 8.2$. The ballistic ($\sim t^2$, dashed line), sub-diffusive ($\sim t^{0.63}$, solid line) and diffusive regimes ($\sim t$, dashed line) are indicated (D is the diffusion coefficient of a chain). Right ordinate: relaxation time $\tau_1(h, T)$ versus $T - T_c(h)$. Results for the bulk and two free-standing films of thicknesses $h \sim 8$ and $h \sim 14$ are shown. Since h decreases on cooling, only an approximate film thickness can be specified. This is meant by the notation '$h \sim 8$' referring to the film with $h = 8$ at $T = 0.44$. The fit curves to equation (5) are shown for the bulk (solid line) and the film with $h \sim 8$ (dotted line); they are labelled by the corresponding exponents $\gamma_1(h)$. Equation (5) gives: $T_c \simeq 0.333$, $\gamma_1 \simeq 2.2$ for $h \sim 8$; $T_c \simeq 0.365$, $\gamma_1 \simeq 2.1$ for $h \sim 14$; $T_c \simeq 0.405$, $\gamma_1 \simeq 1.96$ for the bulk.

not immediately become diffusive. One rather finds a sub-diffusive regime where $g_1(t) \propto t^{0.63}$, which is caused by chain connectivity [31, 33]. The transition to diffusive motion, $g_1(t) \sim t$, only occurs if the MSD exceeds the average chain size (see the data for $h = 8$).

While qualitatively similar, bulk and film dynamics are significantly different at the quantitative level. Figure 1 demonstrates that the relaxation of the films is faster and caging is less pronounced. A slowing down of the film dynamics comparable to that of the bulk is only observed for $T < 0.44$ [31, 33]. Thus, the films at $T = 0.44$ appear to be further away from their glass transition—in other words, the glass transition temperature T_g in the films should be lower than in the bulk.

We may check this interpretation by exploring the T dependence of the relaxation time τ_1 defined through

$$g_1(t = \tau_1(h, T)) = 1. \tag{4}$$

τ_1 is the time it takes a monomer on average to cover the distance of its own size. This is only possible if the monomer succeeds in leaving its nearest-neighbour cage. τ_1 thus belongs to the time regime of the α-relaxation.

We analyse the T dependence of τ_1 in the framework of the ideal mode-coupling theory (MCT) [38, 39]. Ideal MCT predicts that structural relaxation times of a bulk glass-forming system diverge when T approaches a critical temperature T_c from above. Following this prediction for the bulk [38, 39] we attempted to fit τ_1 by a power law of the form

$$\tau_1(h, T) \propto \left(\frac{1}{T - T_c(h)}\right)^{\gamma_1(h)}. \tag{5}$$

From this analysis we find that the value of T_c in the films is smaller than in the bulk and that film and bulk data for τ_1 collapse onto a master curve when plotted versus $T - T_c(h)$ (cf figure 1). This indicates that $T_c(h)$ is an important reference temperature for the slow dynamics in our glass-forming polymer systems. In the next section, we discuss the h dependence of T_c in more detail by comparing this dependence with that of T_g obtained from other computational and experimental studies.

3.2. Thickness dependence of $T_c(h)$ and $T_g(h)$

References [4, 5] propose the following formula for the thickness dependence of $T_g(h)$:

$$T_g(h) = \frac{T_g}{1 + h_0/h}. \tag{6}$$

Here T_g denotes the bulk glass transition temperature and h_0 is a characteristic length scale. Equation (6) results from the assumption that the relaxation in a film close to T_g is determined by the coupling of the viscoelastic bulk to capillary waves at the free surface. This identifies the parameter h_0 as the ratio $h_0 = \gamma/E$ where E is the Young modulus of the film and γ the surface tension at the free surface [4].

Equation (6) suggests a superposition property. Scaling temperature by the bulk T_g (or T_c) and h by h_0 should yield a master curve for experimental and simulation data. Figure 2 demonstrates that this superposition property indeed holds. Besides the $T_c(h)$ results for the studied free-standing films the figure also shows T_c values for supported and confined films for our model [31, 33], Monte Carlo simulation results for T_g for free-standing polypropylene (PP) films from reference [12], and experimental glass transition temperatures for low molecular weight [4] and high molecular weight [1] polystyrene (PS) films supported on silicon wafers. For the high molecular weight films T_g was measured by ellipsometry; for the low molecular weight films two different methods were employed, depending on film thickness. For $h >$ 9.6 nm T_g was also determined by ellipsometry, whereas for smaller thicknesses T_g was inferred from the T dependence of the film viscosity obtained by spinodal dewetting experiments.

The comparison presented in figure 2 suggests three conclusions. First, the results for PS films of low molecular [4] and high molecular weights [43] closely agree with each other. Thus, it seems unlikely that a possible modification of chain entanglement [44–46] or chain conformations [47, 48] in thin films represents the main cause for the observed T_g depression. Second, figure 2 shows that the scaling predicted by equation (6) is robust. It allows us to superimpose computational and experimental results from microscopically very different systems by adapting a single parameter, h_0 (the bulk T_g or T_c are known from independent measurements). h_0 varies weakly from system to system, in the present comparison at most by a factor of about 2 for the supported and free-standing films of the bead-spring model (see also [31] for further discussion). Third, in view of the theoretical justification proposed in [4] the good agreement of equation (6) with the simulation results for confined films is surprising

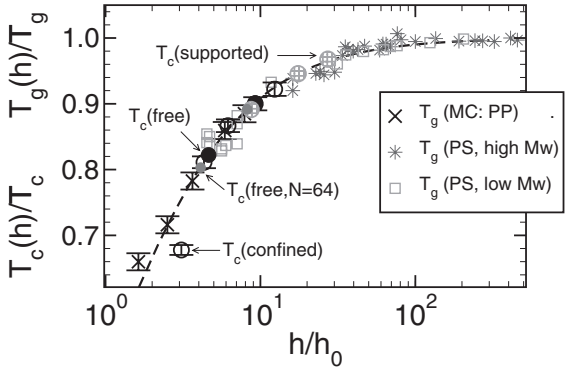

Figure 2. Scaling plot of $T_c(h)$ and $T_g(h)$ following equation (6). $T_c(h)$ is the critical temperature of MCT for $N = 10$ and 64. For $N = 10$ three film geometries are shown: free-standing films (filled circles), supported films (grey hatched circles), confined films (open circles). The results for confined films—the melt is confined between two smooth, repulsive walls—are taken from [40, 41]; those for supported films—the melt is supported by a smooth, weakly attractive substrate on one side and has a polymer–vacuum interface at the opposite side—are taken from [33]. For $N = 64$ only results for free-standing films are shown (grey filled circles). The dashed line presents equation (6) ($N = 10$: $h_0 = 0.76$ for supported films, $h_0 = 1.47$ for free-standing films, and $h_0 = 1.64$ for confined films, bulk $T_c = 0.405$; $N = 64$: $h_0 = 1.68$ for free-standing films, bulk $T_c = 0.415$). Our MD results for T_c are compared to the glass transition temperatures $T_g(h)$ of three studies: (i) Monte Carlo simulations of a lattice model for free-standing atactic polypropylene (PP) films [12] (crosses; $N = 50$; $T_g = 391$ K, $h_0 = 6.1$ Å; 9.95 Å $\leqslant h/2 \leqslant$ 48.1 Å). Both T_g and h_0 are results of a fit to equation (6). (ii) Experiments of supported atactic polystyrene (PS) films (spin cast from toluene solution onto silicon wafers) [4] (squares; $N \simeq 20$, $R_g = 13$ Å; $T_g = 327$ K = bulk T_g for $N = 20$, $h_0 = 8.2$ Å; 38.5 Å $\leqslant h \leqslant$ 1678 Å). (iii) Experiments of supported, high molecular weight PS films [1] (stars; $N \simeq 29\,000$, $R_g \simeq 453$ Å; $T_g = 375$ K, $h_0 = 6.8$ Å [42]; 110 Å $\leqslant h \leqslant$ 3100 Å). The data of [12] are reproduced with permission. The high molecular weight PS data are reproduced from [2] by courtesy of Forrest.

because capillary waves should be suppressed by solid interfaces[3]. This suggests that another mechanism should be responsible for the T_c reduction in this case. In [31, 40, 41] we argued that a modification of the monomer packing at the surface occurs; this is, for instance, reflected by a decrease in the first maximum of the collective structure factor $S(q)$. The decrease of $S(q)$ implies that the nearest-neighbour cage does not tighten on cooling as efficiently as in the bulk, which should lead, according to MCT [39], to faster dynamics.

3.3. Layer-resolved dynamics

The mean square displacement discussed in section 3.1 aggregates contributions from all (middle) monomers, irrespective of their position in the film. Further insight can be obtained by a layer-resolved analysis. Here we introduce the y-dependent MSD $g_0(t, y)$ defined as

$$g_0(t, y) = \left\langle \frac{1}{n_t} \sum_i \prod_{t'=0}^{t} \delta\left[y - y_i(t')\right] |\vec{r}_i^{\,\parallel}(t) - \vec{r}_i^{\,\parallel}(0)|^2 \right\rangle. \tag{7}$$

This definition only takes into account the n_t monomers of a chain which are at all times $t' < t$ within a slab of width Δy whose centre is at a distance y from the surface. The position of

[3] The theoretical justification of equation (6) may raise further questions. For instance, the work of [49–52] indicates that the q dependence of the relaxation rate should be more complicated than expected from the viscoelastic capillary wave model leading to equation (6). Further issues are also discussed in the commentaries [53, 54].

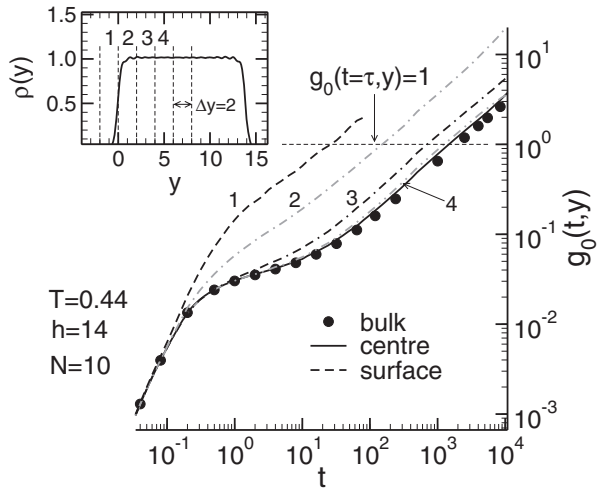

Figure 3. Main figure: layer-resolved MSD $g_0(t, y)$ at $T = 0.44$ for a free-standing film of thickness $h = 14$. y denotes the distance from the Gibb's dividing surface (situated at $y = 0$). Only displacements parallel to the wall are considered for the films (lines); the bulk data (•) are multiplied by $2/3$ to put them on the same scale as the film data. $g_0(t, y)$ is obtained as an average over all monomers of a chain which remain for all times shown in a layer of width $\Delta y = 2$ that is centred at y (equation (7)). Eventually, monomers will leave the layer in which they were initially. This gives rise to a loss of statistical accuracy at long t; the data are thus sometimes truncated at late times where large statistical noise occurred. The dashed horizontal line indicates the definition of the local relaxation time $\tau(y, T)$ (equation (8)). Inset: corresponding monomer density profile $\rho(y)$ versus y. The layers for which $g_0(t, y)$ is shown in the main figure are labelled by numbers (1, 2, 3, 4).

the surface (i.e. of the origin $y = 0$) is identified with the Gibbs dividing surface [33]. As before, we only consider motion in the unconstrained parallel directions in order to allow for a comparison with the bulk. Equation (7) averages over all monomers of a chain—instead of focusing only on the middle monomer as in equation (3)—because the layer-wise resolution of the dynamics is statistically very demanding.

Figure 3 depicts $g_0(t, y)$ for a film of thickness $h = 14$ at $T = 0.44$ ($T_c(h) = 0.365$). The figure reveals a pronounced dependence of the monomer dynamics on the distance from the free surface. While $g_0(t, y)$ displays a two-step relaxation—characteristic of the cold melt close to T_c—in the centre, this feature is gradually lost on approaching the surface, and is absent at the surface. Similar results are found in other simulations [12, 14, 16, 21]; our findings also agree qualitatively with the results of fluorescence [9] and NMR experiments [5].

It is tempting to try to correlate the layer dependence of $g_0(t, y)$ to the monomer density profile $\rho(y)$ (cf inset of figure 3). Since the average monomer density decreases on approaching the free surface, this could give rise to faster relaxation. However, while the low density is certainly an important factor for the fast dynamics in the surface layer (layer '1'), figure 3 suggests that a one to one correspondence between $\rho(y)$ and $g_0(t, y)$ is too simplified. For instance, the density of layers '2' and '3' is already bulk-like, whereas the corresponding $g_0(t, y)$ is larger than the bulk MSD. Apparently, surface effects penetrate into the film more deeply for the monomer MSD than for the monomer density (see [31] for a fuller discussion).

In the following we want to focus on the penetration depth of the surface effects for the dynamics and explore its T dependence. To this end, we define a local relaxation time through

$$g_0(t = \tau(y, T), y) = 1. \tag{8}$$

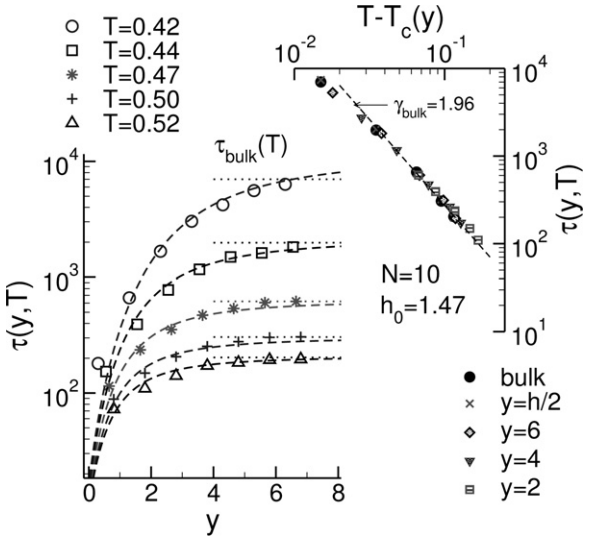

Figure 4. Left ordinate: layer-resolved relaxation time $\tau(y, T)$ for $N = 10$ and various T versus distance y from the Gibbs dividing surface (GDS) for a free-standing film with $h \sim 14$. y is defined as the distance of the centre of a layer from the GDS. The thickness of a layer is $\Delta y = 1$. $\tau(y, T)$ is defined by equation (8). The dotted horizontal lines indicate the bulk value $\tau_{\text{bulk}}(T)$. The dashed lines represent equation (11) where $T_c(y)$ is computed from equation (10). Right ordinate: $\tau(y, T)$ as a function of the reduced temperature $T - T_c(y)$ in different layers of the films. The dashed line indicates equation (11). The bulk results are also included.

$\tau(y, T)$ measures the time it takes a monomer to move across its own size parallel to the wall, provided the monomer is in a layer at distance y from the wall.

Figure 4 shows the results of this analysis for $h \sim 14$ at various temperatures. Not unexpectedly, we find that $\tau(y, T)$ is small at the free surface and increases towards the bulk value with increasing y. Upon cooling, wall effects penetrate further and further into the film. In previous work on confined films [31] and films with a free surface [33], we tried to extract a growing length scale from the range over which $\tau(y, T)$ deviates near the interface from bulk behaviour. The analysis used an empirical formula suggested in [19]. We found that a drawback of this approach was that it was not always possible to unambiguously identify a growing length scale because other fit parameters could also increase (strongly) on cooling [33]. Therefore, we suggest a different approach here which does not introduce a length scale, but associates a different critical temperature $T_c(y)$ with each layer at distance y from the interface.

Our approach is based on two assumptions. First, we presume that the average $T_c(h)$ of the film can be written as an arithmetic mean of $T_c(y)$. That is,

$$T_c(h) = \frac{2}{h} \int_0^{h/2} \mathrm{d}y\, T_c(y). \tag{9}$$

Here we integrate from the position of the free surface (i.e. of the Gibbs dividing surface) to $h/2$ because a free-standing film is symmetric about its centre. Then using equation (6) one can determine $T_c(y)$ by differentiation. This gives

$$T_c(y) = \frac{T_c(1 + \frac{h_0}{y})}{(1 + \frac{h_0}{2y})^2}. \tag{10}$$

The second hypothesis is that the sole effect of the surface is to shift T_c from the bulk value to $T_c(y)$. We thus postulate that the position and temperature dependent relaxation time $\tau(y, T)$

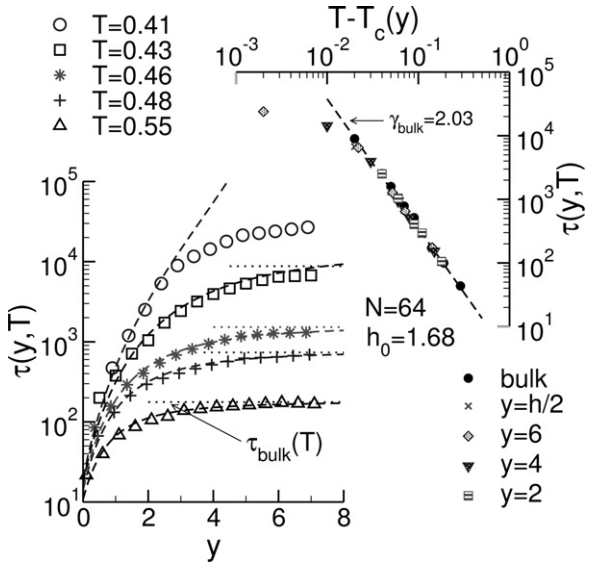

Figure 5. Left ordinate: layer-resolved relaxation time $\tau(y, T)$ for $N = 64$ and various T versus distance y from the Gibbs dividing surface (GDS) for a free-standing film with $h \sim 15$. y is defined as the distance of the centre of a layer from the GDS. The thickness of a layer is $\Delta y = 1$. $\tau(y, T)$ is defined by equation (8). The dotted horizontal lines indicate the bulk value $\tau_{\text{bulk}}(T)$. The dashed lines represent equation (11) where $T_c(y)$ is computed from equation (10). Right ordinate: $\tau(y, T)$ as a function of the reduced temperature $T - T_c(y)$ in different layers of the films. The dashed line indicates equation (11). The bulk results are also included.

can be expressed as

$$\tau(y, T) = \frac{a_{\text{bulk}}}{(T - T_c(y))^{\gamma_{\text{bulk}}}}. \tag{11}$$

For $N = 10$ all parameters of equations (10) and (11) are known from previous studies [33] ($h_0 = 1.47$; $T_c = 0.405$, $a_{\text{bulk}} = 3.01$ and $\gamma_{\text{bulk}} = 1.96$). This allows for a direct comparison between the prediction and simulation. Figure 4 depicts the results of this comparison. For all T shown the y dependence of $\tau(y, T)$ is very well described by equation (11). Only if the distance from the surface becomes comparable to the thickness of the layer the MSDs are calculated in do deviations arise. This is the case here for $y \leqslant 1$. Additionally, it can be seen from the inset that the slowing down within the different layers of the film is indeed bulk-like upon replacing the bulk T_c by $T_c(y)$. This supports our initial assumption, equation (9).[4]

The results presented in figure 4 are not an exception. To demonstrate that, we extended our analysis to longer chains, $N = 64$. This extension of the simulations also provide a hint at the chain length dependence of h_0 and T_c. First, we determined the input parameters of equations (10) and (11) from bulk simulations and the thickness dependence of $T_c(h)$. For $N = 64$ we obtain $h_0 = 1.68$; $T_c = 0.415$, $a_{\text{bulk}} = 3.3$ and $\gamma_{\text{bulk}} = 2.03$. As expected, T_c is (slightly) larger than for $N = 10$ ($T_c = 0.405$). However, from the experimental results (cf figure 2) one should expect h_0 to decrease with increasing N. We found the opposite trend. Nevertheless, figure 5 shows that we can again describe $\tau(y, T)$ by equation (11) over the whole y and T range, except for the lowest temperature $T = 0.41$. Contrary to the analysis for $N = 10$, this temperature is below the bulk critical temperature $T_c = 0.415$. Close to T_c the

[4] Note that although $T_c(h)$ seems to be an arithmetic mean of $T_c(y)$, this is not the case for the relaxation time, i.e. $\tau(h, T) \neq \frac{2}{h} \int_0^{h/2} \mathrm{d}y\, \tau(y, T)$, because $\tau(h, T)$ is a nonlinear function of $T_c(h)$.

MCT approximation for the relaxation time breaks down (see e.g. [31] for a detailed discussion of this point) and thus also equation (11) cannot be expected to reproduce the simulation data. This deviation is also visible in figure 4 for the lowest studied temperature, $T = 0.42$.

4. Conclusions

When a supported or free-standing polymer film is confined to nanoscopic dimensions its glass transition temperature can be depressed relative to the bulk value [28, 29]. It appears natural to assume—and simulations suggest [12, 14, 16, 21]—that monomers in contact with the free surface are less constrained and thus more mobile than in the bulk. One may thus hypothesize that the observed T_g reductions are caused by a liquid-like surface layer [1]. There is experimental evidence supporting this idea. For instance, NMR experiments by Herminghaus *et al* suggest that there is a well-defined molten layer at the surface of a thin film of nonentangled polystyrene (PS) chains [5]. Similar results are also obtained for highly entangled PS chains by Ellison and Torkelson [9]. By means of a fluorescence/multilayer technique they conclude that there is a continuous reduction of T_g on approaching the free surface.

In this paper we provided further evidence for these experimental observations by molecular dynamics simulations of a bead-spring model. We studied nonentangled ($N = 10$) and slightly entangled ($N = 64$) chains in a temperature regime above the critical temperature T_c of mode-coupling theory. For both chain lengths we find that the film dynamics is spatially heterogeneous. Monomers at the free surface relax faster than they would in the bulk at the same temperature T. The relaxation transitions from enhanced to bulk dynamics with increasing distance y from the surface. For all T the crossover to bulk dynamics remains smooth, but its range grows on cooling. This gradient in the relaxation dynamics may be associated with a gradient of critical temperatures $T_c(y)$. Here $T_c(y)$ is not a fit parameter; its distance dependence can be derived from two ingredients. First, we assume that $T_c(h)$—the global T_c for a film of thickness h—is the arithmetic mean of $T_c(y)$. Second, we use the result that the depression of $T_c(h)$ with decreasing h, found in our simulations, can be well described by equation (6), an expression suggested in [4] for the reduction of T_g in supported PS films.

The local $T_c(y)$ thus obtained appears to be an important reference point for the layer-resolved dynamics in our model. When plotting the local relaxation time $\tau(y, T)$ versus the reduced temperature $T - T_c(y)$ we find a master curve for all layers which coincides with the increase of the bulk relaxation time on cooling toward the the bulk T_c (see figures 4 and 5). Individual layers thus behave as if they were a bulk system with reduced critical temperature. This suggests that the different T dependence of the bulk and film-averaged relaxation times (see figure 1) is probably due to 'dynamic heterogeneities' between the layers and not due to a growing heterogeneity within a given layer relative to the bulk. Our results further suggest that the heterogeneity between the layers increases upon cooling because layers close to the film centre experience a stronger slowing down than surface layers which are still quite far from their respective $T_c(y)$.

Acknowledgments

We have presented results from the groups of W L Mattice and J A Forrest. We are grateful that they quickly provided the figures requested. Our simulations were made possible by generous grants of computer time at the IDRIS (Orsay). We acknowledge financial support from the European Community's 'Marie-Curie Actions' under contract MRTN-CT-2004-504052 (POLYFILM) and from the IUF.

References

[1] Keddie J L, Jones R A L and Cory R A 1994 *Europhys. Lett.* **27** 59
[2] Forrest J A and Dalnoki-Veress K 2001 *Adv. Colloid Interface Sci.* **94** 167
[3] Sharp J, Teichroeb J and Forrest J 2004 *Eur. Phys. J.* **15** 473
[4] Herminghaus S, Jacobs K and Seemann R 2001 *Eur. Phys. J.* E **5** 531
[5] Herminghaus S, Seemann R and Landfester K 2004 *Phys. Rev. Lett.* **93** 017801
[6] Seemann R *et al* 2005 *J. Phys.: Condens. Matter* **17** S267
[7] Grohens Y *et al* 2002 *Eur. Phys. J.* E **8** 217
[8] Kim J H, Jang J and Zin W-C 2001 *Langmuir* **17** 2703
[9] Ellison C J and Torkelson J M 2003 *Nat. Mater.* **2** 695
[10] Ellison C, Mundra M and Torkelson J 2005 *Macromolecules* **38** 1767
[11] Alba-Simionesco C *et al* 2003 *Eur. Phys. J.* E **12** 19
[12] Xu G and Mattice W L 2003 *J. Chem. Phys.* **118** 5241
[13] Starr F W, Schrøder T B and Glotzer S C 2001 *Phys. Rev.* E **64** 021802
[14] Riggleman R A, Yoshimoto K, Douglas J F and de Pablo J J 2006 *Phys. Rev. Lett.* **97** 045502
[15] Yoshimoto K, Jain T S, Nealey P F and de Pablo J J 2005 *J. Chem. Phys.* **122** 144712
[16] Böhme T R and de Pablo J J 2002 *J. Chem. Phys.* **116** 9939
[17] Baljon A R C, VanWeert M H M, Barber DeGraaff R and Khare R 2005 *Macromolecules* **38** 2391
[18] Baljon A R C, Billen J and Khare R 2004 *Phys. Rev. Lett.* **93** 255701
[19] Scheidler P, Kob W and Binder K 2004 *J. Phys. Chem.* B **108** 6673
[20] Teboul V and Alba-Simionesco C 2002 *J. Phys.: Condens. Matter* **14** 5699
[21] Morita H *et al* 2006 *Macromolecules* **39** 6233
[22] de Gennes P G 2000 *Eur. Phys. J.* E **2** 201
[23] McCoy J D and Curro J G 2002 *J. Chem. Phys.* **116** 9154
[24] Mittal J, Shah P and Truskett T M 2004 *J. Phys. Chem.* B **108** 19769
[25] Long D and Lequeux F 2001 *Eur. Phys. J.* E **4** 371
[26] Ngai K L 2003 *Eur. Phys. J.* E **12** 93
[27] Oyerokum F T and Schweizer K S 2005 *J. Chem. Phys.* **123** 224901
[28] Roth C B and Dutcher J R 2005 *Soft Materials: Structure and Dynamics* ed J R Dutcher and A G Marangoni (New York: Dekker) pp 1–38
[29] Alcoutlabi M and McKenna G B 2005 *J. Phys.: Condens. Matter* **17** R461
[30] Alba-Simionesco C *et al* 2006 *J. Phys.: Condens. Matter* **18** R15
[31] Baschnagel J and Varnik F 2005 *J. Phys.: Condens. Matter* **17** R851
[32] Donth E 2001 *The Glass Transition* (Berlin: Springer)
[33] Peter S, Meyer H and Baschnagel J 2006 *J. Polym. Phys.* B **44** 2951
[34] Baschnagel J, Wittmer J P and Meyer H 2004 *Computational Soft Matter: From Synthetic Polymers to Proteins* (*NIC Series (Jülich)* vol 23) ed N Attig, K Binder, H Grubmüller and K Kremer, pp 83–140, available from http://www.fz-juelich.de/nic-series
[35] Kremer K and Grest G S 1990 *J. Chem. Phys.* **92** 5057
[36] Pütz M, Kremer K and Grest G S 2000 *Europhys. Lett.* **49** 735
see also Pütz M, Kremer K and Grest G S 2000 *Europhys. Lett.* **52** 719 (Comment)
Pütz M, Kremer K and Grest G S 2000 *Europhys. Lett.* **52** 721 (Reply)
[37] Jakobsen A 2005 *J. Chem. Phys.* **122** 124901
[38] Götze W 1999 *J. Phys.: Condens. Matter* **11** A1
[39] Chong S-H and Fuchs M 2002 *Phys. Rev. Lett.* **88** 185702
[40] Varnik F, Baschnagel J and Binder K 2002 *Phys. Rev.* E **65** 021507
[41] Varnik F, Baschnagel J and Binder K 2002 *Eur. Phys. J.* E **8** 175
[42] Kim J H, Jang J and Zin W-C 2000 *Langmuir* **16** 4067
[43] Forrest J A, Dalnoki-Veress K and Dutcher J R 1997 *Phys. Rev.* E **56** 5705
[44] Bernazzani P, Simon S L, Plazek D J and Ngai K L 2002 *Eur. Phys. J.* E **8** 201
[45] Tsui O K C and Zhang H F 2001 *Macromolecules* **34** 9139
[46] Si L *et al* 2005 *Phys. Rev. Lett.* **94** 127801
[47] Cavallo A *et al* 2005 *J. Phys.: Condens. Matter* **17** S1697
[48] Müller M 2002 *J. Chem. Phys.* **116** 9930
[49] Jäckle J and Kawasaki K 1995 *J. Phys.: Condens. Matter* **7** 4351
[50] Jäckle J 1998 *J. Phys.: Condens. Matter* **10** 7121
[51] Kim H *et al* 2003 *Phys. Rev. Lett.* **90** 068302
[52] Madsen A *et al* 2004 *Phys. Rev. Lett.* **92** 096104
[53] Long D 2002 *Eur. Phys. J.* E **8** 245
[54] Baschnagel J 2002 *Eur. Phys. J.* E **8** 247